

# Competing Unconventional Charge-Density-Wave States in Cuprate Superconductors: Spin-Fluctuation-Driven Mechanism

Kouki Kawaguchi<sup>1</sup>, Youichi Yamakawa<sup>1</sup>, Masahisa Tsuchiizu<sup>2</sup>, and Hiroshi Kontani<sup>1</sup>

<sup>1</sup> *Department of Physics, Nagoya University, Furo-cho, Nagoya 464-8602, Japan.*

<sup>2</sup> *Department of Physics, Nara Women's University, Nara 630-8506, Japan*

(Dated: June 5, 2018)

To understand the origin of unconventional charge-density-wave (CDW) states in cuprate superconductors, we establish the self-consistent CDW equation, and analyze the CDW instabilities based on the realistic Hubbard model, without assuming any  $\mathbf{q}$ -dependence and the form factor. Many higher-order many-body processes, which are called the vertex corrections, are systematically generated by solving the CDW equation. When the spin fluctuations are strong, the uniform  $\mathbf{q} = \mathbf{0}$  nematic CDW with  $d$ -form factor shows the leading instability. The axial nematic CDW instability at  $\mathbf{q} = \mathbf{Q}_a = (\delta, 0)$  ( $\delta \approx \pi/2$ ) is the second strongest, and its strength increases under the static uniform CDW order. The present theory predicts that uniform CDW transition emerges at a high temperature, and it stabilize the axial  $\mathbf{q} = \mathbf{Q}_a$  CDW at  $T = T_{\text{CDW}}$ . It is confirmed that the higher-order Aslamazov-Larkin processes cause the CDW orders at both  $\mathbf{q} = \mathbf{0}$  and  $\mathbf{Q}_a$ .

Keywords: charge-density-wave, cuprate high- $T_c$  superconductors, pseudogap, nematicity

The origin and the nature of the complex electronic states in cuprate high- $T_c$  superconductors are central unsolved issues in condensed matter physics. Recently, interesting interplay between the magnetism, nematicity, and superconductivity has been revealed by many experiments. Figure 1 (a) shows the schematic phase diagram of hole-doped cuprate superconductors. Strong spin fluctuations develop for wide doping and temperature ranges, and short-range spin fluctuations are the origin of various non-Fermi-liquid-like electronic states (such as the  $T$ -linear resistivity and  $T^{-1}$  behavior of the Hall coefficient) and the  $d$ -wave superconductivity at  $T_c \sim 100$  K [1–4]. However, the microscopic origin of the nematicity has been unsolved. For example, at  $T = T_{\text{CDW}}$ , the axial charge-density-wave (CDW) at wavevector  $\mathbf{q} = \mathbf{Q}_a = (\delta, 0)$  ( $\delta \approx \pi/2$ ), which is parallel to the nearest Cu-Cu direction, is observed by the X-ray scattering studies [5–12], STM studies [13–16], and local lattice deformation [17]. The band-folding due to the CDW should suppress the density-of-states and spin fluctuations.

There are many open problems on the nature of the pseudogap phase below  $T^*$ , such as whether it is a distinct phase or a continuous crossover. Recently, strong evidences for the nematic transition at  $T^*$  have been reported by the resonant ultrasound spectroscopy [18], ARPES analysis [19], and magnetic torque measurement [20]. Fundamental questions for theorists are: what is the order parameter of the nematic phase below  $\sim T^*$ , and why the nematic CDW is realized inside the pseudogap phase. The mean-field-level approximations, such as the random-phase-approximation (RPA), cannot explain any CDW instabilities unless sizable inter-site Coulomb interactions are introduced [21, 22]. Thus, we study the role of the vertex corrections (VCs) that describes the strong charge-spin interference [23–27].

The idea of the “spin-fluctuation-driven CDW” due to

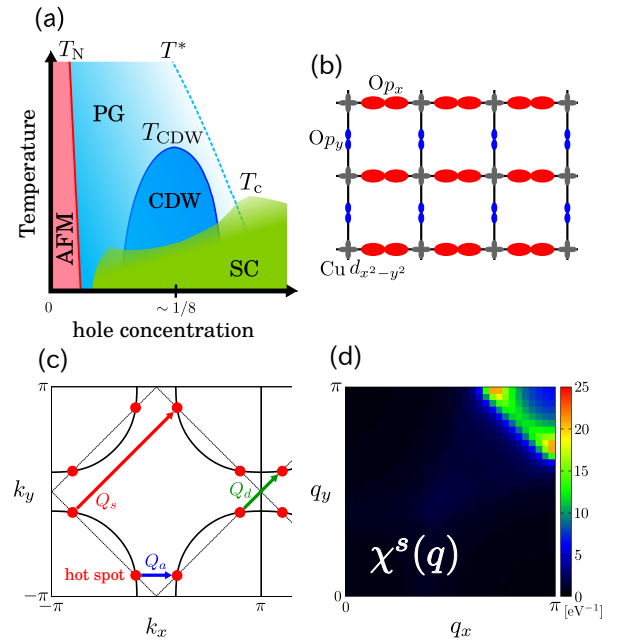


FIG. 1: (color online) (a) Schematic phase diagram of hole-doped cuprates with the pseudogap (PG), charge-density-wave (CDW), antiferromagnetism (AFM), and superconductivity (SC).  $T^*$  is the pseudogap temperature and  $T_{\text{CDW}}$  is the CDW temperature. (b)  $\mathbf{q} = \mathbf{0}$  CDW due to  $p$ -orbital polarization ( $n_x \neq n_y$ ) in real space. (c) FS of the  $d$ - $p$  Hubbard model for  $n = 4.9$ . (d)  $\chi^s(\mathbf{q})$  for  $U = 4.06$  eV.

the VCs has been studied intensively [23, 27–32]. By developing this idea, the electronic nematic phases in Fe-based superconductors [23], Ru-oxides [24], and cuprate superconductors [28–33] have been explained. The irreducible VC derived from the Ward-identity ( $\delta\hat{\Sigma}/\delta\hat{G}$ ) within the one-loop approximation is given by the single- and double-fluctuation terms, respectively called the Maki-Thompson (MT) and Aslamazov-Larkin (AL) VCs

(see Fig. 2 (b)). As studied in Ref. [28], the higher-order MT processes give the diagonal CDW with  $\mathbf{q} = \mathbf{Q}_d = (\delta, \delta)$ , which is, however, inconsistent with experiments. The axial CDW is given by the lowest-order AL process if small inter-site Coulomb interaction exists [22]. However, the uniform nematic order that corresponds to the pseudogap phase is failed to be explained. Therefore, new theoretical method should be developed.

In this paper, we establish the self-consistent CDW equation, and analyze the CDW instabilities based on the  $d$ - $p$  Hubbard model. By solving the CDW equation, higher-order VCs given by the repetition of the AL and MT processes are systematically included, without assuming any  $\mathbf{q}$ -dependence and the form factor. When the spin fluctuations are strong, we obtain the uniform CDW with  $p$ -orbital polarization ( $n_x \neq n_y$ ), which is schematically shown in Fig. 1 (b). This uniform  $p$ -orbital polarization strongly enlarges the axial nematic CDW instability at  $\mathbf{q} = \mathbf{Q}_a$ . The present study leads to the prediction that the uniform  $p$ -orbital polarization occurs at  $T^*$ , and axial  $\mathbf{q} = \mathbf{Q}_a$  CDW is induced at  $T_{\text{CDW}} < T^*$ . We verified that the higher-order AL processes are significant for the rich CDW orders in under-doped cuprates.

We analyze the three-orbital  $d$ - $p$  model  $H = H_0 + H_U$  introduced in Ref. [22]: The kinetic term is  $H_0 = \sum_{\mathbf{k}, \sigma} \hat{c}_{\mathbf{k}, \sigma}^\dagger \hat{h}_{\mathbf{k}} \hat{c}_{\mathbf{k}, \sigma}$ , where  $\hat{c}_{\mathbf{k}, \sigma}^\dagger \equiv (d_{\mathbf{k}, \sigma}^\dagger, p_{x, \mathbf{k}, \sigma}^\dagger, p_{y, \mathbf{k}, \sigma}^\dagger)$ , and  $\hat{h}_{\mathbf{k}}$  is the first-principles tight-binding model for  $\text{La}_2\text{CuO}_4$  [34] with the additional 3rd-nearest  $d$ - $d$  hopping  $t_{dd}^{\text{3rd}} = -0.1$  eV. The Fermi surface (FS) for the electron filling  $n = n_d + n_p = 4.9$  shown in Fig. 1 (c) is similar to the hole-like FS in Y- and Bi-based cuprates. In the interaction term  $H_U$ , we introduce only the  $d$ -orbital on-site Coulomb interactions  $U$ . In the RPA, the spin (charge) susceptibility for the  $d$ -orbital is  $\chi^{s(c)}(q) = \chi^0(q)/(1 - (+)U\chi^0(q))$ , where  $q \equiv (\mathbf{q}, \omega_l)$  and  $\omega_l = 2l\pi T$ . Here,  $\chi^0(q) = -T \sum_{\mathbf{k}} G(\mathbf{k} + \mathbf{q})G(\mathbf{k})$  is the bare bubble, and  $G(\mathbf{k}) = (\hat{1}(i\epsilon_n - \mu) - \Delta\hat{\Sigma}(\mathbf{k}) - \hat{h}_{\mathbf{k}})_{1,1}^{-1}$  is the Green function for the  $d$ -orbital. Here,  $\mathbf{k} \equiv (\mathbf{k}, \epsilon_n)$ ,  $\epsilon_n = (2n+1)\pi T$ , and  $\Delta\Sigma(\mathbf{k})$  is the symmetry-breaking self-energy; we will introduce later. Figure 1 (d) shows the obtained spin susceptibility for  $\Delta\Sigma(\mathbf{k}) = 0$ , in the case of  $U = 4.06$  eV,  $n = 4.9$  and  $T = 50$  meV. The spin Stoner factor  $\alpha_S \equiv \max_{\mathbf{q}}\{U\chi^0(\mathbf{q})\}$  is 0.99. Hereafter, we fix the parameters  $n = 4.9$  and  $T = 50$  meV.

In principle, the CDW order parameter is given as the ‘‘symmetry breaking in the self-energy’’, similarly to the superconductivity given as the symmetry-breaking in the anomalous self-energy. In Ref. [35], we developed the symmetry-breaking self-energy method, and explained the nematic orbital order in Fe-based superconductors. The non-magnetic nematic order with the sign-reversing orbital polarization in  $\mathbf{k}$ -space in FeSe has been satisfactorily explained [35]. Here, we apply the same method to analyze the CDW in cuprates. The symmetry-breaking

self-energy equation is given as

$$\Delta\Sigma(\mathbf{k}) = (1 - P_{A_{1g}})T \sum_{\mathbf{q}} \left( \frac{3}{2}V^s(\mathbf{q}) + \frac{1}{2}V^c(\mathbf{q}) - U^2\chi^0(\mathbf{q}) \right) \times G(\mathbf{k} + \mathbf{q}), \quad (1)$$

where  $V^s(\mathbf{q}) = U + U^2\chi^s(\mathbf{q})$ ,  $V^c(\mathbf{q}) = -U + U^2\chi^c(\mathbf{q})$ , and  $G(\mathbf{k})$  contains the symmetry-breaking term  $\Delta\Sigma$ .  $P_{A_{1g}}$  is the  $A_{1g}$  symmetry projection operator. This equation is shown in Fig. 2 (a). In the FeSe model, the nonzero solution  $\Delta\Sigma \neq 0$  with the  $B_{1g}$  symmetry at  $\mathbf{q} = \mathbf{0}$  is obtained for  $\alpha_S \geq 0.82$  [35]. In order to study the CDW at  $\mathbf{q} \neq \mathbf{0}$ , however, we have to calculate Eq. (1) for the large cluster model.

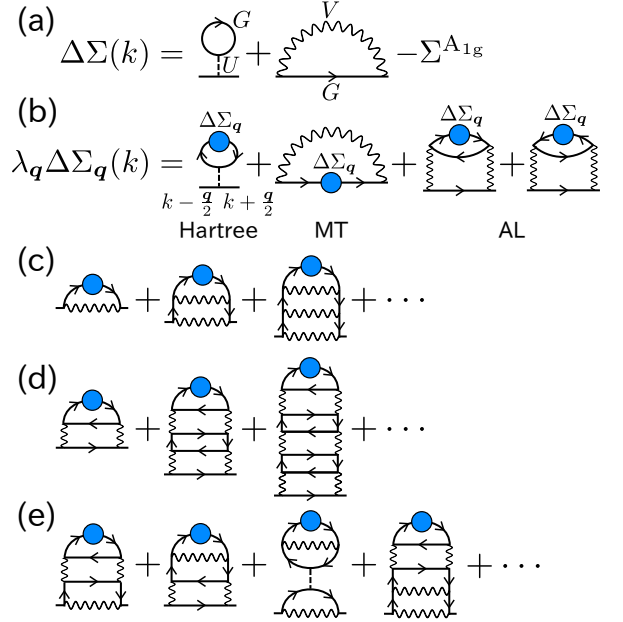


FIG. 2: (color online) (a) Schematic self-consistent equation for the CDW order parameter.  $\Delta\Sigma$  is the symmetry-breaking self-energy that represents the CDW order. (b) Schematic linearized CDW order equation for general wavenumber  $\mathbf{q}$ . (c) Higher-order MT processes. (d) Higher-order AL processes. (e) Examples of the mixture of different processes.

In order to analyze the CDW state with arbitrary wavevector  $\mathbf{q}$ , we introduce the linearized CDW equation by linearizing Eq. (1) with respect to  $\Delta\Sigma$ . The obtained equation is

$$\lambda_{\mathbf{q}} \Delta\Sigma_{\mathbf{q}}(\mathbf{k}) = T \sum_{\mathbf{k}'} K(\mathbf{q}; \mathbf{k}, \mathbf{k}') \Delta\Sigma_{\mathbf{q}}(\mathbf{k}'), \quad (2)$$

where  $\lambda_{\mathbf{q}}$  is the eigenvalue for the CDW at  $\mathbf{q}$ . When the maximum of  $\lambda_{\mathbf{q}}$  reaches unity at  $\mathbf{q}$ , Eq. (1) for the sufficiently large cluster model has nonzero solution, and the eigenvector  $\Delta\Sigma_{\mathbf{q}}(\mathbf{k})$  gives the CDW form factor. The kernel  $K(\mathbf{q}; \mathbf{k}, \mathbf{k}')$  is given as

$$K(\mathbf{q}; \mathbf{k}, \mathbf{k}') = \left( \frac{3}{2}V_0^s(\mathbf{k} - \mathbf{k}') + \frac{1}{2}V_0^c(\mathbf{k} - \mathbf{k}') \right)$$

$$\begin{aligned}
& \times G_0(k' + \mathbf{q}/2)G_0(k' - \mathbf{q}/2) \\
& -T \sum_p \left( \frac{3}{2} V_0^s(p + \mathbf{q}/2)V_0^s(p - \mathbf{q}/2) \right. \\
& \quad \left. + \frac{1}{2} V_0^c(p + \mathbf{q}/2)V_0^c(p - \mathbf{q}/2) \right) \\
& \times G_0(k - p) (\Lambda_{\mathbf{q}}(k'; p) + \Lambda_{\mathbf{q}}(k'; -p)), \quad (3)
\end{aligned}$$

where  $\Lambda_{\mathbf{q}}(k; p) \equiv G_0(k + \frac{\mathbf{q}}{2})G_0(k - \frac{\mathbf{q}}{2})G_0(k - p)$ . The subscript 0 in Eq. (3) represents the functions with  $\Delta\Sigma = 0$ . (In Eq. (3), we should subtract the double-counting term in the  $U^2$ -order.) The diagrammatic expression for Eqs. (2)-(3) is shown in Fig. 2 (b): The kernel  $K(\mathbf{q}; k, k')$  contains the Hartree term, the MT term, and the two AL terms. Both the MT term and the AL terms may drive the spin-fluctuation-driven CDW. The AL terms drives the  $\mathbf{q} = \mathbf{0}$  CDW instability since its functional form  $\propto \sum_{\mathbf{k}} \chi^s(\mathbf{k} + \mathbf{q})\chi^s(\mathbf{k})$  is large for  $\mathbf{q} \approx \mathbf{0}$  [23, 36]. Although the Hartree term suppress the CDW instability in single-orbital models, its suppression disappears if the form factor has sign-reversal.

By solving the linearized equation, the higher-order diagrams with respect to these terms are generated. For instance, we show the higher-order MT and AL processes in Figs. 2 (c) and (d), respectively. The examples of different processes are given in Fig. 2 (e).

Hereafter, we analyze the linearized CDW equation in Eq. (2) numerically. Here, we drop the  $\epsilon_n$ -dependence of  $\Delta\Sigma_{\mathbf{q}}(k)$  by performing the analytic continuation  $i\epsilon_n \rightarrow \epsilon$  and putting  $\epsilon = 0$ . We also neglect the  $\epsilon_n$ -dependent self-energy due to spin fluctuations in the kernel  $K(\mathbf{q}; k, k')$ . Due to these simplifications, the obtained  $\lambda_{\mathbf{q}}$  is expected to be overestimated. Therefore, we do not put the constraint  $\lambda_{\mathbf{q}} < 1$  in the numerical study. We will show below that  $\lambda_{\mathbf{q}}$  is actually reduced by introducing the constant damping  $\gamma$  in Green functions (not in  $V_0^{s,c}(q)$ ) in Eq. (3).

Figure 3 (a) shows the  $\mathbf{q}$ -dependence of the eigenvalue  $\lambda_{\mathbf{q}}$  obtained for  $\gamma = 0.1 \sim 0.5$  eV when  $\alpha_S = 0.995$  at  $T = 50$ meV. Here,  $\lambda_{\mathbf{q}}$  is the largest at  $\mathbf{q} = \mathbf{0}$ , meaning that the uniform CDW emerges at the highest temperature. As shown in Fig. 3 (b), the corresponding form factor  $\Delta\Sigma_{\mathbf{0}}(\mathbf{k})$  has the  $d$ -wave symmetry, resulting in the uniform  $p$ -orbital polarization with  $n_{px} \neq n_{py}$  shown in Fig. 1 (b). The second largest peak appears at  $\mathbf{q} = \mathbf{Q}_a = (\delta, 0)$ , which corresponds to the axial CDW. Its form factor  $\Delta\Sigma_{\mathbf{Q}_a}(\mathbf{k})$  is  $s$ -wave like, shown in Fig. 3 (c). Since these form factors have sign reversal in  $\mathbf{k}$ -space, the contribution from the Hartree term in Eq. (3) (Fig. 2 (b)) is absent or negligibly small. That is, the present CDW fluctuations driven by the VCs originate from the irreducible part of the charge susceptibility with respect to  $U$ , since the reducible part is negligible due to the sign-reversing form factor.

To find the origin of the CDW instability, we solve the linearized CDW equation by including only two AL

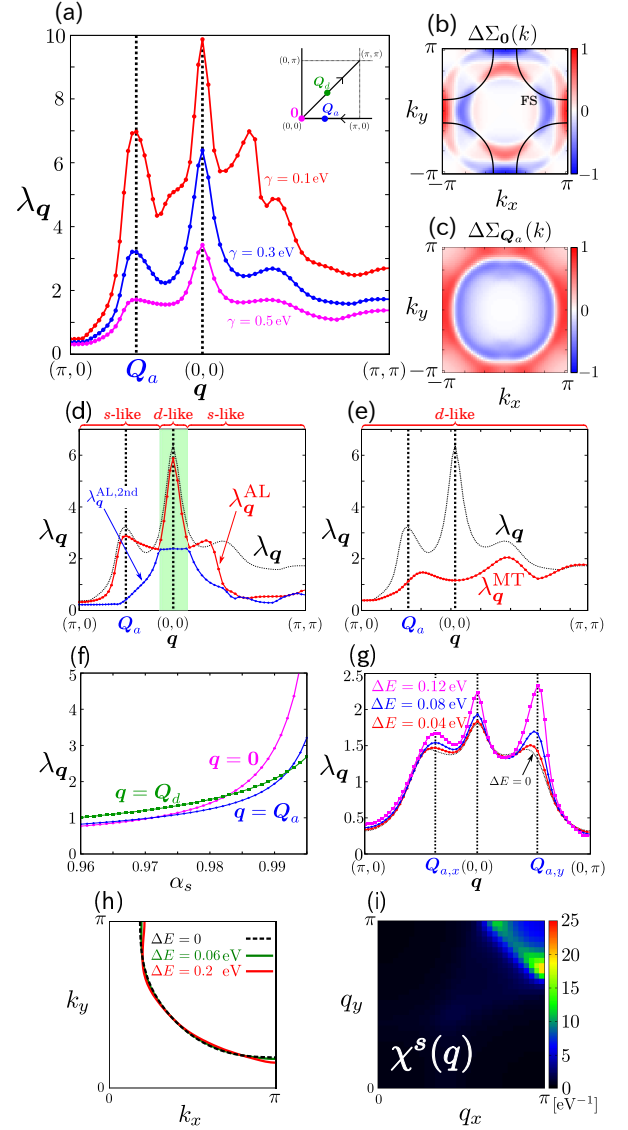


FIG. 3: (color online) (a)  $\mathbf{q}$ -dependence of  $\lambda_{\mathbf{q}}$  obtained for  $\gamma = 0.1 \sim 0.5$  eV. (b) Form factor for  $\mathbf{q} = \mathbf{0}$  ( $d$ -wave) normalized by its maximum value. (c) Form factor for  $\mathbf{q} = \mathbf{Q}_a = (\delta, 0)$  ( $s$ -wave like). (d)  $\lambda_{\mathbf{q}}^{\text{AL}}$  given by including only the AL processes for  $\gamma = 0.3$  eV.  $\lambda_{\mathbf{q}}^{\text{AL},2\text{nd}}$  is the second largest eigenvalue. (e)  $\lambda_{\mathbf{q}}^{\text{MT}}$  given by including only the MT processes. (f)  $\lambda_{\mathbf{q}}$  at  $\mathbf{q} = \mathbf{0}$ ,  $\mathbf{Q}_a$  and  $\mathbf{Q}_d$  as function of  $\alpha_S$ . (g)  $\lambda_{\mathbf{q}}$  under the uniform nematic CDW order for  $\Delta E = 0 \sim 0.12$ eV. (h) The deformed FS for  $\Delta E = 0.06$  eV and  $0.2$  eV. (i)  $\chi^s(\mathbf{q})$  for  $\Delta E = 0.06$ eV.

terms (MT term) in  $K(\mathbf{q}; k, k')$ ; see Fig. 2 (b), and denote the obtained eigenvalue as  $\lambda_{\mathbf{q}}^{\text{AL(MT)}}$ . In Fig. 3 (d), we show  $\lambda_{\mathbf{q}}^{\text{AL}}$  (and the second-largest eigenvalue  $\lambda_{\mathbf{q}}^{\text{AL},2\text{nd}}$ ), for  $\alpha_S = 0.995$  and  $\gamma = 0.3$ eV. At  $\mathbf{q} = \mathbf{0}$  and  $\mathbf{Q}_a$ ,  $\lambda_{\mathbf{q}}^{\text{AL}}$  is almost equal to the true eigenvalue  $\lambda_{\mathbf{q}}$  shown by the broken line. The form factor for  $\lambda_{\mathbf{q}}^{\text{AL}}$  is  $d$ -wave only for  $\mathbf{q} \approx \mathbf{0}$ , shown by the shaded area. Outside this area, the  $d$ -wave eigenvalue decreases and replaced with the  $s$ -wave solution. In contrast,  $\lambda_{\mathbf{q}}^{\text{MT}}$  shown in Fig. 3 (e)

is much smaller than  $\lambda_{\mathbf{q}}$  at  $\mathbf{q} = \mathbf{0}$  and  $\mathbf{Q}_a$ , whereas  $\lambda_{\mathbf{q}}$  at  $\mathbf{q} = \mathbf{Q}_d = (\delta, \delta)$  is comparable to the true eigenvalue. Therefore, the CDW instabilities at  $\mathbf{q} = \mathbf{0}$  and  $\mathbf{Q}_a$  originate from the AL processes, whereas the instability at  $\mathbf{q} = \mathbf{Q}_d$  is mainly derived from the MT processes.

Figure 3 (f) shows the eigenvalues at  $\mathbf{q} = \mathbf{0}$ ,  $\mathbf{Q}_a$ , and  $\mathbf{Q}_d$  as function of  $\alpha_S$ . When the spin fluctuations are smaller ( $\alpha_S \lesssim 0.98$ ),  $\lambda_{\mathbf{q}}$  has the maximum at  $\mathbf{q} = \mathbf{Q}_d$ , since the spin-fluctuation-driven VCs are small. As the spin fluctuations increases,  $\lambda_{\mathbf{q}}$  is drastically enlarged by the VCs, and  $\lambda_{\mathbf{0}}$  becomes the largest due to the AL processes. The relation  $\lambda_{\mathbf{Q}_a} > \lambda_{\mathbf{Q}_d}$  is realized for  $\alpha_S \gtrsim 0.99$ .

Hereafter, we study the linearized CDW equation under the static uniform CDW order;  $\Delta E(\mathbf{k}) = \Delta E \times \Delta \Sigma_{\mathbf{0}}(\mathbf{k})$ , where  $\Delta \Sigma_{\mathbf{0}}(\mathbf{k})$  is normalized by its maximum value. That is,  $\max_{\mathbf{k}} \{\Delta E(\mathbf{k})\} = \Delta E$ . Figure 3 (g) shows the eigenvalues for  $\Delta E = 0 \sim 0.12$  eV at  $U = 4.04eV$ . For  $\Delta E \geq 0.1eV$ ,  $\lambda_{\mathbf{q}}$  at  $\mathbf{q} = \mathbf{Q}_{a,y} = (0, \delta)$  is larger than the eigenvalues at  $\mathbf{q} = \mathbf{0}$  and  $\mathbf{Q}_{a,x} = (\delta, 0)$ . Thus, the axial CDW instability is magnified by the nematic FS deformation under the uniform CDW order. Figures 3 (h) and (i) show the  $C_2$ -symmetric FSs and  $\chi^s(\mathbf{q})$ , respectively. For  $\Delta E = 0.06$  eV, the change in the filling is  $(\Delta n_d, \Delta n_{p_x}, \Delta n_{p_y}) = (-0.034, -0.179, +0.213) \times 10^{-3}$ . The prominent  $C_2$ -symmetric spin susceptibility is consistent with the neutron study for under-doped YBCO [37].

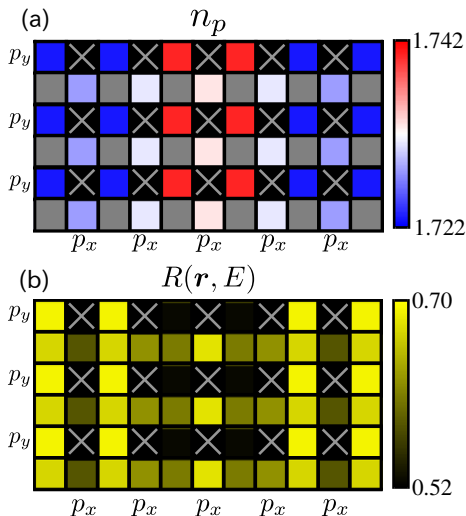


FIG. 4: (color online) (a)  $\Delta n_{p_x}$  and  $\Delta n_{p_y}$  on O sites in the CDW state given by the form factor at  $\mathbf{q} = (\pi/2, 0)$  for  $\Delta E = 0.4eV$ . No atoms exist at the cross sites. (b)  $R(\mathbf{r}, E) = I(\mathbf{r}, E)/I(\mathbf{r}, -E)$  for  $E = 0.5$  eV at Cu and O sites, which is similar to the STM data [14, 16].

The form factor  $\Delta \Sigma_{\mathbf{q}}(\mathbf{k})$  gives the modulation of the charge density in real space. Since the  $d$ -wave form factor at  $\mathbf{q} = \mathbf{0}$  represents the bond order  $t_{dd}^x \neq t_{dd}^y$ , it gives the orbital polarization  $n_{p_x} \neq n_{p_y}$  shown in Fig. 1 (b). Figure 4 (a) shows the  $p$ -orbital polarization derived from

the axial CDW form factor  $\Delta E(\mathbf{k}) \propto \Delta \Sigma_{\mathbf{Q}_{a,x}}(\mathbf{k})$  with  $\Delta E = 0.4$  eV. Although the form factor in Fig. 3 (c) is  $s$ -wave like, the obtained  $p$ -orbital polarization is antiphase between the nearest  $p_x$  and  $p_y$  sites ( $d$ -wave type). We also calculate the ratio  $R(\mathbf{r}, E) = I(\mathbf{r}, E)/I(\mathbf{r}, -E)$ , where  $I(\mathbf{r}, E) = \int_0^E N(\mathbf{r}, E') dE'$  is the tunneling current in the STM study. The obtained result for  $E = 0.5eV$  is shown in Fig. 4 (b), which reproduces the characteristic STM pattern reported in Refs. [14, 16].

In Ref. [22], we have shown that the axial CDW order at  $\mathbf{q} = (\delta, 0)$ , by considering the lowest-order AL process and introducing small inter-site Coulomb interaction  $V_{dp}$ . The obtained  $\delta$  decreases with the hole-doping in proportion to the wavelength between the hot spots [22]. On the other hand, the axial CDW order is obtained even if  $V_{dp} = 0$  by the functional-renormalization-group (fRG) analysis [27]. The present study clarified that the higher-order AL processes in Fig. 2 (d) causes divergent CDW instabilities at  $\mathbf{q} = \mathbf{0}$  and  $\mathbf{Q}_a$  even for  $V_{dp} = 0$ . Recently, we improved the numerical accuracy of the fRG method at  $\mathbf{q} \sim \mathbf{0}$ , and verified that the uniform CDW instability is the strongest [38], consistently with the present theory.

The pseudogap phenomena under  $T^*$ , such as the Fermi arc formation [39–41], remains unsolved since the uniform CDW cannot account for the pseudogap. We consider that the short-range spin-fluctuations at  $T \sim T^*$  induces not only the uniform CDW due to the AL processes, but also the large quasiparticle damping [42–44], and the latter causes the pseudogap behaviors. It is also our important future issue to explain the doping dependence of  $T^*$ ,  $T_{CDW}$  and  $T_c$  quantitatively by improving the theoretical method.

In summary, we analyzed the linearized CDW equation based on the  $d$ - $p$  Hubbard model, by including both the MT and AL VCs into the kernel. When the spin fluctuations are strong ( $\alpha_S \gtrsim 0.98$ ), the uniform nematic CDW has the strongest instability. The axial CDW instability is strongly magnified under the uniform CDW order, even if the deformation of the FS is small. These results lead to the prediction that the uniform  $p$ -orbital polarization occurs at  $\sim T^*$ , and axial  $\mathbf{q} = \mathbf{Q}_a$  CDW is shown in Fig. 1 (a) is induced at  $T_{CDW} < T^*$ . We verified that the higher-order AL processes give the rich CDW orders. Various rich spin-fluctuation-driven charge orders (such as the CDW and orbital order) are caused by the VCs not only in cuprate and Fe-based superconductors, but also other metals near the magnetic criticality.

We are grateful to S. Onari, Y. Matsuda, T. Hanaguri, T. Shibauchi, Y. Kasahara, and Y. Gallais for fruitful discussions. This study has been supported by Grants-in-Aid for Scientific Research from MEXT of Japan.

[1] T. Moriya and K. Ueda, Adv. Phys. **49**, 555 (2000).



- [2] K. Yamada: *Electron Correlation in Metals* (Cambridge Univ. Press 2004).
- [3] D. J. Scalapino, Phys. Rep. **250**, 329 (1995).
- [4] H. Kontani, Rep. Prog. Phys. **71**, 026501 (2008); H. Kontani, *Transport Phenomena in Strongly Correlated Fermi Liquids* (Springer-Verlag Berlin and Heidelberg GmbH & Co. K, 2013).
- [5] G. Ghiringhelli, M. L. Tacon, M. Minola, S. Blanco-Canosa, C. Mazzoli, N. B. Brookes, G. M. D. Luca, A. Frano, D. G. Hawthorn, F. He, T. Loew, M. M. Sala, D. C. Peets, M. Salluzzo, E. Schierle, R. Sutarto, G. A. Sawatzky, E. Weschke, B. Keimer, and L. Braicovich, Science **337**, 821 (2012).
- [6] J. Chang, E. Blackburn, A. T. Holmes, N. B. Christensen, J. Larsen, J. Mesot, R. Liang, D. A. Bonn, W. N. Hardy, A. Watenphul, M. v. Zimmermann, E. M. Forgan, and S. M. Hayden, Nature Physics **8**, 871 (2012).
- [7] E. Blackburn, J. Chang, M. Hücker, A. T. Holmes, N. B. Christensen, R. Liang, D. A. Bonn, W. N. Hardy, U. Rütt, O. Gutowski, M. v. Zimmermann, E. M. Forgan, and S. M. Hayden, Phys. Rev. Lett. **110**, 137004 (2013).
- [8] R. Comin, A. Frano, M. M. Yee, Y. Yoshida, H. Eisaki, E. Schierle, E. Weschke, R. Sutarto, F. He, A. Soumyanarayanan, Y. He, M. L. Tacon, I. S. Elfimov, J. E. Hoffman, G. A. Sawatzky, B. Keimer, and A. Damascelli, Science **343**, 390 (2014).
- [9] E. H. da Silva Neto, P. Aynajian, A. Frano, R. Comin, E. Schierle, E. Weschke, A. Gyenis, J. Wen, J. Schneeloch, Z. Xu, S. Ono, G. Gu, M. L. Tacon, and A. Yazdani, Science **343**, 393 (2014).
- [10] W. Tabis, Y. Li, M. L. Tacon, L. Braicovich, A. Kreyssig, M. Minola, G. Dellea, E. Weschke, M. J. Veit, M. Ramazanoglu, A. I. Goldman, T. Schmitt, G. Ghiringhelli, N. Barišić, M. K. Chan, C. J. Dorow, G. Yu, X. Zhao, B. Keimer, and M. Greven, Nature Commun. **5**, 5875 (2014).
- [11] M. Hücker, M. v. Zimmermann, G. D. Gu, Z. J. Xu, J. S. Wen, G. Xu, H. J. Kang, A. Zheludev, and J. M. Tranquada, Phys. Rev. B **83**, 104506 (2011).
- [12] R. Comin, R. Sutarto, F. He, E. da Silva Neto, L. Chauviere, A. Frano, R. Liang, W. N. Hardy, D. Bonn, Y. Yoshida, H. Eisaki, J. E. Hoffman, B. Keimer, G. A. Sawatzky, and A. Damascelli, Nature Materials **14**, 796 (2015).
- [13] T. Hanaguri, C. Lupien, Y. Kohsaka, D.-H. Lee, M. Azuma, M. Takano, H. Takagi, and J. C. Davis, Nature **430**, 1001 (2004).
- [14] Y. Kohsaka, T. Hanaguri, M. Azuma, M. Takano, J. C. Davis, and H. Takagi, Nature Physics **8**, 534 (2012).
- [15] M. J. Lawler, K. Fujita, J. Lee, A. R. Schmidt, Y. Kohsaka, C. K. Kim, H. Eisaki, S. Uchida, J. C. Davis, J. P. Sethna, and E.-A. Kim, Nature **466**, 347 (2010).
- [16] K. Fujita, M. H. Hamidian, S. D. Edkins, C. K. Kim, Y. Kohsaka, M. Azuma, M. Takano, H. Takagi, H. Eisaki, S. Uchida, A. Allais, M. J. Lawler, E.-A. Kim, S. Sachdev, and J. C. S. Davis, Proc. Natl. Acad. Sci. USA, **110**, E3026 (2014).
- [17] A. Bianconi, N. L. Saini, A. Lanzara, M. Messori, and T. Rossetti, H. Oyanagi, H. Yamaguchi, K. Oka, and T. Ito, Phys. Rev. Lett. **76**, 3412 (1996).
- [18] A. Shekhter, B. J. Ramshaw, R. Liang, W. N. Hardy, D. A. Bonn, F. F. Balakirev, R. D. McDonald, J. B. Betts, S. C. Riggs, and A. Migliori, Nature **498**, 75 (2013).
- [19] Rui-Hua He, M. Hashimoto, H. Karapetyan, J. D. Koralek, J. P. Hinton, J. P. Testaud, V. Nathan, Y. Yoshida, Hong Yao, K. Tanaka, W. Meevasana, R. G. Moore, D. H. Lu, S.-K. Mo, M. Ishikado, H. Eisaki, Z. Hussain, T. P. Devereaux, S. A. Kivelson, J. Orenstein, A. Kapitulnik, and Z.-X. Shen, Science **331**, 1579 (2011).
- [20] Y. Sato, Y. Kasahara, T. Shibauchi and Y. Matsuda, private communication
- [21] S. Bulut, W.A. Atkinson and A.P. Kampf, Phys. Rev. B **88**, 155132 (2013).
- [22] Y. Yamakawa, and H. Kontani, Phys. Rev. Lett. **114**, 257001 (2015).
- [23] S. Onari and H. Kontani, Phys. Rev. Lett. **109**, 137001 (2012).
- [24] M. Tsuchiizu, Y. Ohno, S. Onari, and H. Kontani, Phys. Rev. Lett. **111**, 057003 (2013).
- [25] S. Onari, Y. Yamakawa, and H. Kontani, Phys. Rev. Lett. **112**, 187001 (2014).
- [26] H. Kontani and Y. Yamakawa, Phys. Rev. Lett. **113**, 047001 (2014).
- [27] M. Tsuchiizu, Y. Yamakawa, and H. Kontani, Phys. Rev. B **93**, 155148 (2016).
- [28] M.A. Metlitski and S. Sachdev, New J. Phys. **12**, 105007 (2010); S. Sachdev and R. La Placa, Phys. Rev. Lett. **111**, 027202 (2013).
- [29] C. Husemann and W. Metzner, Phys. Rev. B **86**, 085113 (2012); T. Holder and W. Metzner, Phys. Rev. B **85**, 165130 (2012).
- [30] Y. Wang and A.V. Chubukov, Phys. Rev. B **90**, 035149 (2014).
- [31] J. C. S. Davis and D.-H. Lee, Proc. Natl. Acad. Sci. USA, **110**, 17623 (2013).
- [32] E. Berg, E. Fradkin, S. A. Kivelson, and J. M. Tranquada, New J. Phys. **11**, 115004 (2009).
- [33] P. P. Orth, B. Jeevanesan, R. M. Fernandes, and J. Schmalian, arXiv:1703.02210.
- [34] P. Hansmann, N. Parragh, A. Toschi, G. Sangiovanni, and K. Held, New J. Phys. **16**, 033009 (2014).
- [35] S. Onari, Y. Yamakawa, and H. Kontani, Phys. Rev. Lett. **116**, 227001 (2016).
- [36] S. Caprara, C. Di Castro, M. Grilli, and D. Suppa, Phys. Rev. Lett. **95**, 117004 (2005).
- [37] V. Hinkov, D. Haug, B. Fauque, P. Bourges, Y. Sidis, A. Ivanov, C. Bernhard, C. T. Lin, and B. Keimer, Science, **319**, 597 (2008).
- [38] M. Tsuchiizu, K. Kawaguchi, Y. Yamakawa, and H. Kontani, unpublished.
- [39] T. Yoshida, X. J. Zhou, T. Sasagawa, W. L. Yang, P. V. Bogdanov, A. Lanzara, Z. Hussain, T. Mizokawa, A. Fujimori, H. Eisaki, Z.-X. Shen, T. Kakeshita, and S. Uchida, Phys. Rev. Lett. **91**, 027001 (2003); M. Hashimoto, I. M. Vishik, Z.-X. Shen, and A. Fujimori, J. Phys. Soc. Jpn. **81**, 011006 (2012).
- [40] A. Kanigel, M. R. Norman, M. Randeria, U. Chatterjee, S. Souma, A. Kaminski, H. M. Fretwell, S. Rosenkranz, M. Shi, T. Sato, T. Takahashi, Z. Z. Li, H. Raffy, K. Kadowaki, D. Hinks, L. Ozyuzer and J. C. Campuzano, Nature Physics **2**, 447 (2006).
- [41] T. Kondo, Y. Hamaya, A. D. Palczewski, T. Takeuchi, J. S. Wen, Z. J. Xu, G. Gu, J. Schmalian, and A. Kaminski, Nature Physics **7**, 21 (2011).
- [42] D. Senechal and A.-M.S. Tremblay, Phys. Rev. Lett. **92**, 126401 (2004).
- [43] B. Kyung, S. S. Kancharla, D. Senechal, A. -M. S. Tremblay, M. Civelli, and G. Kotliar, Phys. Rev. B **73**, 165114

- (2006).
- [44] T.A. Maier, M.S. Jarrell, and D.J. Scalapino, *Physica C*, **460-462**, 13 (2007).